December 1985 INT 125/85

MEASUREMENTS OF ELECTROMAGNETIC COUPLING IN THE ION CYCLOTRON FREQUENCY RANGE FROM AN EXTERNAL ANTENNA TO A LOW DENSITY PLASMA

M.L. Sawley and P.J. Paris

MEASUREMENTS OF ELECTROMAGNETIC COUPLING IN THE ION CYCLOTRON FREQUENCY RANGE FROM AN EXTERNAL ANTENNA TO A LOW DENSITY PLASMA

M.L. Sawley and P.J. Paris

Centre de Recherches en Physique des Plasmas
Association Euratom - Confédération Suisse
Ecole Polytechnique Fédérale de Lausanne
21, Av. des Bains, CH-1007 Lausanne, Switzerland

ABSTRACT

Coupling from an external antenna to the low density, magnetized plasma of the LMP device has been experimentally investigated in the frequency range $\omega \simeq \omega_{ci}$. An azimuthal magnetic wavefield, which is not present in the absence of plasma, has been observed. The amplitude of this field exhibits a resonance for $\omega \simeq \omega_{ci}$. Comparison is given between observations and the predictions of a fluid model.

I. INTRODUCTION

The studies described in this report were motivated by a proposed investigation of the nonlinear modification of the ion concentration ratio due to a large amplitude wave in a magnetized, two ion species plasma (Weibel, 1980). An outline of this proposed project has been given by Tran et al. (1982). The basic idea consists of exciting in a cylindrical plasma column a standing electromagnetic wave whose amplitude varies along the axis of the column. The axial ponderomotive force exerted by the wave on a given species i changes sign as the wave frequency ω crosses the cyclotron frequency ω_{ci} of that species (Motz and Watson, 1967). If the wave frequency is situated between the ion cyclotron frequencies in a two ion species plasma, the ponderomotive force acts to concentrate the lighter species near the spatial maximum of the electric field of the wave and the heavier species near the spatial minimum. This effect is largest for $\omega \simeq \omega_{ci}$, and therefore for two ions with similar mass (Festeau-Barrioz and Sawley, 1985).

Before nonlinear effects such as described above can be studied, it is necessary to ensure that a suitable wavefield of sufficient amplitude may be excited within the plasma column. For a plasma of sufficently low density, the self consistent currents induced within the plasma will not be large enough to shield the near field of an external antenna from penetrating into the plasma column (Sawley, 1985). A study of the ponderomotive force acting under these conditions is described by Muggli (1984). Alternatively, it may be possible to excite an eigenmode of the colunm which, provided that the damping is not excessive, will enable a large amplitude field to co-exist with the plasma. It is the excitation of an eigenmode with $\omega \simeq \omega_{ci}$ in a low density plasma that is the subject of this report.

A theoretical study of bounded ion cyclotron waves in a cylindrical cavity partially filled with a two ion species plasma has been described by Sawley and Tran (1982). Calculations were made for parameter values relevant to the experiment described here. An MHD model of the waves was adopted, with the major damping mechanism

assumed to be ion-neutral collisions. Coupling of power from an external "Stix coil" antenna to the various axial and radial eigenmodes was considered. From this calculation, the power required to excite a particular wavefield of the amplitude needed for nonlinear studies could be determined.

The present work can therefore be regarded as an experimental test of the assumptions underlying the theory of Sawley and Tran (1982). An electromagnetic wavefield is excited within the plasma column by passing an oscillating current through the external antenna. The wavefield is measured by inserting magnetic probes into the plasma. Using phase-locked techniques, fields of very low amplitude could be detected. Substantial differences between the experiment and the predictions of theory have been found. These differences may be accounted for by the effects of electron Landau damping and anomalous (turbulence-enhanced) collisional damping of the excited waves.

It should be noted that ion cyclotron waves have been extensively studied in the past, in particular due to their application to plasma heating (see, for example, references listed in Sawley and Tran, 1982). However, these experiments have been conducted on plasmas of significantly higher densities than that of the present study. Consequently, the waves launched had substantially different characteristics, being of much shorter axial wavelength and essentially electromagnetic in nature. Conversely, the waves studied in the present experiment have a very long axial wavelength, and exhibit (theoretically) a strong electrostatic behaviour, even though the small associated magnetic field proved to be of sufficient amplitude to be detected.

II. EXPERIMENTAL APPARATUS

The experiments described here were conducted on the Linear Magnetized Plasma (LMP) device. Design studies for this machine commenced in 1980, with completion and the first plasma in June 1982. Following the construction and testing of the wave launching antenna,

the results described in this report were obtained in the first months of 1984.

The LMP creates a cylindrical plasma column of length 4.75 m and diameter 5 cm, using a gas discharge between a heated barium oxide coated cathode located at one end of the device and a plate anode located at the other. A uniform (<0.3%) axial magnetic field, B_0=3 kG for the present study, is created by passing a d.c. current through a water-cooled solenoid surrounding the plasma column. A schematic diagram of the LMP is shown in Fig. 1. Further details of the device may be obtained from Tran et al. (1982).

II.1 Plasma properties

For the present experiments a neon plasma was used. Naturally occuring neon (≈ 90% Ne^{20}, 10% Ne^{22}) provided a suitable two ion species plasma, as analyzed in the calculations of Sawley and Tran (1982). The filling gas pressure was maintained in the range of 1.5 to 3.5×10^{-4} torr by feedback control of a piezo-electric inlet value. A d.c. discharge current was maintained in the range of 0.2 to 6.0 A. This created a plasma with $10^{10} \leq n_e \leq 8\times10^{11}$ cm^{-3}, as measured by a 33 GHz microwave interferometer located 1 m from the cathode, following the empirical law :

$$n_e / p_0 I_{cathode} \simeq 3.9\times10^{14} \text{ cm}^{-3}/\text{torr amp.}$$

The percentage ionization of the plasma formed was less than 5%. The electron temperature, measured by Langmuir probes situated at various axial locations, was in the range $6 \leq T_e \leq 12$ eV. Typical electron density and temperature profiles shown in Fig. 2, indicate that these quantities are quite uniform across the plasma cross-section, although the density has inevitable gradients near the plasma boundary. The electron temperature was measured to vary by less than 50% along the length of the machine. Although not directly measured, the axial gradient of the electron density is assumed to be of the same order as that of the electron temperature. The relative densities of the two ion species were measured using Doppler-free, two photon, laser

induced fluorescence spectroscopy (Kohler, 1986). Within the measurement error, the concentration of ions is the same as that of neutral atoms. This is to be expected, due to the close similarity of ionization cross-sections for atoms of the two neon isotopes. The ion temperature was measured by laser-induced fluorescence spectroscopy to be $T_i \lesssim 0.2$ eV.

II.2 Wave excitation

The wavefield in the plasma was produced using a Stix coil surrounding the column, as described by Sawley and Tran (1982). This antenna consists of four separate coil modules, alternately dephased by 180° (by reversing the direction of current flow) and placed at regular intervals along the machine. Each module is 67.5 cm in length and 12 cm in diameter, while the spacing between the centres of neighbouring modules is 135 cm. Each module consists of 24 turns of square section copper tubing separated into six sub-coils and joined by straight sections. This design was chosen to avoid reducing the diagnostic access to the region beneath the coil modules, the sub-coils being aligned beneath the main magnetic field coils of the LMP device. The design includes a Faraday shield between the wave coils and the plasma. The shield was constructed from a copper tube of thickness ≈ 1 mm (at 200 kHz, skin depth ≈ 0.2 mm), with eight equally-spaced axial cuts along almost the entire length (Dodge et al., 1966). The Faraday shield was observed to be necessary to avoid spurious electrostatic coupling to the plasma due to the inductive voltage drop along the length of each coil module. Without the Faraday shield there was also observed evidence of arcing along the coils, this being eliminated by the presence of the shield. Each module of the Stix coil was individually water cooled, allowing for steady state operation. The antenna was driven, via a capacitor matching circuit, by a 1 kW solid state amplifier (ENI model 1140 LA, flat gain for 9 kHz < f < 250 kHz). The antenna circuit, including connections and matching circuit, was found to have a resistance of approximately 1.5 Ω. This allowed an oscillating current of maximum amplitude $I_{rf} = 50$ A to be driven in the antenna. Figure 3(a) gives a schematic diagram of the antenna and matching circuit construction. A more detailed diagram of a coil module is shown in Fig. 3(b).

II.3 Wave detection

The magnetic wavefield was detected by pick-up coils positioned at various axial locations along the LMP device. These probes could be moved to yield radial profiles of the wavefield. Each probe was constructed by winding 60 turns of 0.05 mm diameter insulated wire on a mica former 0.15 mm × 1.0 mm. The resulting probes were calibrated using a Helmholtz coil. They had an effective area of NA ≃ 8×10^{-5} m^2, yielding a unintegrated signal of ≃ 10 mV/gauss for a frequency of 200 kHz. In order to detect low signal levels, a phase-locked detection system was used. The probe output after pre-amplification was fed into a high frequency lock-in (PAR Model 5202). The current in the antenna coils was used to calibrate the phase of the reference signal. Phase shifts that may have been introduced by the probe, pre-amplifier or cables were corrected for in the lock-in circuitry. The in-phase and quadrature outputs of the lock-in were recorded, yielding the in-phase and out-of-phase amplitudes of the magnetic wavefield. Figure 4 shows a schematic diagram of the probe detection system.

An attempt was also made, using a capacitive double probe, to measure the electric field of the wave excited in the plasma. While a deal of effort was taken to shield properly the probe shaft from electrostatic pick-up, it was noticed that this probe was very sensitive to plasma noise and to the proximity of the antenna coils. Thus meaningful measurements of the electric field in the presence of theplasma could not be obtained.

It should be noted that for the low density plasma considered, there is not a significant power input to the plasma : the vast majority of the available 1 kW amplifier power is dissipated in the resistance of the antenna, matching circuit, leads and connections. It is therefore not possible to detect plasma coupling via a change in the antenna impedance.

III EXPERIMENTAL RESULTS

III.1 General observations

The following points could be noted from the magnetic probe measurements :

(i) Beneath a coil module, the magnetic field was essentially axial, i.e., b_z. It was not possible to measure an azimuthal component, b_θ, in the vicinity of the antenna coils, due to the problem caused by a small probe misalignment or nonuniformity of the probe windings.

(ii) For the plasma parameters considered, there was no noticeable change in b_z beneath a coil module introduced by the presence of a plasma.

(iii) Away from the coil module (that is, at an axial distance greater than the decay length of the vacuum field), the magnetic field was essentially azimuthal. The small b_z field detected was at least an order of magnitude smaller, and may have been due to stray pick-up.

(iv) When measuring b_θ, there was always (except at very large distances $\gtrsim$ 50 cm from a coil module) a signal detected without plasma, due to electrical pick-up. The values of b_θ shown below are the difference between signals recorded with and without plasma. For some circumstances, the resulting value may be smaller than the signal without plasma. However, whenever it was much less (i.e., $< {}^1/_{10}$), it became unreliable and was therefore discarded. This only occurred very close to a coil module ($\lesssim$ 10 cm away).

(v) When the probe was rotated through 180°, the signal (with - without plasma) changed sign. This is an indication that the probe was actually measuring the magnetic field, and not just electrical pick-up.

(vi) The lock-in system described in section II.3 was capable of measuring very small field amplitudes (resolution $\lesssim$ 1 mgauss).

(vii) All the measurements presented here were obtained with a d.c. plasma, although it is possible to use the lock-in system with a pulsed plasma if the pulse length is > 5 ms.

(viii) The probe signals were not filtered or integrated. However, since the frequency is fixed by that of the coil current, and both in-phase and out-of-phase signals are monitored, it is straightforward to obtain the field amplitude and phase.

III.2 Wave measurements

Since in the absence of plasma, the azimuthal magnetic field is everywhere zero (assuming that the antenna current is purely azimuthal, as ideally imagined), a coupling to the plasma from the antenna can be implied by measuring an azimuthal field in the presence of the plasma. This is most readily undertaken at an axial position midway between two coil modules. Figure 5 shows the results of such a measurement, using a probe located between the first and second coil module, $\simeq$ 1 m from the cathode. The probe was positioned at the mid-radius value, r = 1.25 cm. The in-phase component is plotted for four different values of cathode current (and therefore plasma density, since $n_e \propto I_{cathode}$) in Fig. 5(a), and the out-of-phase component in Fig. 5(b).

From Fig. 5(a) it can be noticed that there is a resonance in the in-phase component of b_θ in the vicinity of the cyclotron frequency of the majority (Ne^{20}) ion species. The width of the resonance appears to be quite large, with a full width at half amplitude of $\simeq$ 40 kHz. Both the resonance frequency and width appear to be independent of plasma density. No noticable effect occurs at the cyclotron frequency of the minority (Ne^{22}) species. Figure 5(b) shows that the out-of-phase component of b_θ increases strongly as the frequency passes from below $\omega_c(Ne^{22})$ to above $\omega_c(Ne^{20})$. Again, the

form of the curves obtained appears to be independent of plasma density.

That the observed resonance and increase of the in-phase and out-of-phase components of b_θ are dependent on the ion cyclotron frequency is demonstrated in Fig. 6. In this figure is shown the results of similar measurements obtained with a slightly lower value of B_0. (It can be assumed that there is little change in the plasma parameters, e.g., n, T, for this small change in B_0.) The resonance is seen again at the cyclotron frequency of the majority species.

The dependence of b_θ(r=1.25cm) for f = 220 kHz on plasma density is shown in Fig. 7. For $I_{cathode} > 500mA$ (and the neutral pressure indicated), the wavefield amplitude is proportional to the plasma density without a significant change in phase.

Both the in-phase and out-of-phase components of b_θ increase with neutral pressure, as shown in Fig. 8. At the highest pressures considered, the in-phase signal shows signs of saturation. This may be caused by an increase in damping due to ion-neutral collisions. For the range of parameters considered, $n_e \propto p_0 I_{cathode}$, however $\nu_{in} \propto p_0$ but independent of $I_{cathode}$.

Radial profiles of b_θ(f=220kHz) measured midway between two coil modules is shown in Fig. 9. The profile of the in-phase component plotted in Fig. 9(a) resembles a distorted $J_1(k_\perp r)$ Bessel function. (The distortion presumably being the result of density gradients in the vicinity of the plasma edge : see Fig. 2.) On axis, the in-phase component is zero, consistent with an m = 0 mode. Conversely, the out-of-phase component shown in Fig. 9(b) has a maximum on axis, consistent with an odd m mode. (This may be due to coupling to the plasma of the $m \neq 0$ component of the antenna current associated with the slight assymetry in the design of the coil modules.) The radial profile of b_θ is independent of plasma density. Figure 10(a) shows that the radial profile of the in-phase component of b_θ is also independent of frequency. However, there appears to be significant changes in the radial profile of the out-of-phase component with

frequency, as shown in Fig. 10(b). In fact, for the highest frequency considered, the profile resembles that of an m = 0 mode.

Measurements were also made by exciting only one coil module (third from cathode) and measuring the signal on magnetic probes situated at various distances (towards the cathode) from the module. The dependences of the in-phase and out-of-phase components of b_θ were shown to have the same forms as for the excitation of four modules. In principle, by exciting only one module, it is possible to measure the phase velocity and attenuation length of any waves launched. However, the measurements made could not be interpreted simply in this matter. In fact, there appeared to be present in the plasma a combination of both propagating and standing waves, due presumably to the long damping length (compared to the machine length) of the waves launched. The standing waves could be eliminated by using a short pulse of r.f. current to the coil module. However, for such excitation, it is not possible to use the sensitive phase-locked detection system : the resultant noise problems render useful measurements impossible.

IV. DISCUSSION

Comparing the results presented in section III with the theory of Sawley and Tran (1982), the following points may be noted :

(i) The observation of a magnetic field between coil modules that is almost entirely azimuthal is consistent with the excitation of a bounded ion cyclotron mode as described by Sawley and Tran (1982). In fact, the theory predicts that the radial and axial magnetic wavefield components have a node at the mid-module position, whereas the azimuthal wavefield has an antinode.

(ii) The theory predicts that in the plasma column

$$|b_\theta| \propto \frac{\delta}{\omega k_\parallel} A_1 \quad ,$$

where A_1 is a coefficient proportional to the antenna current. Since, for the plasma parameters of the experiment,

$k_\parallel$ is independent of n_e and $\mathcal{L} \propto \omega_{pe}^2 \propto n_e$, then $b_\theta \propto n_e$. This is confirmed by the experiment, as shown in Fig. 7.

(iii) The azimuthal magnetic field of the ion cyclotron wave is predicted by the theory to exhibit a maximum in the in-phase component, and a change in sign of the out-of-phase component, if an eigenmode is excited (see Fig. 11). Thus, the frequency response of the measured b_θ (shown in Fig. 5) agrees qualitatively with the excitation of an ion cyclotron eigenmode.

(iv) The width of the resonance curves shown in Fig. 5(a) is, however, too broad to be explained solely by ion-neutral collisions. For the parameters considered, the full width of $b_\theta(r=1.25cm,\omega)$ at half amplitude has a theoretical value of $\simeq$ 1.5 kHz (Fig. 11), which is significantly less than the measured value of $\simeq$ 40 kHz. In addition, the amplitude of b_θ measured experimentally is much less than theoretically predicted. One possible explanation is that experimentally the damping of the ion cyclotron wave is enhanced by the presence of plasma turbulence. It should be noted that the neon plasmas generated in the LMP device tend to have a significant level of fluctuations, $\Delta n_e/n_e \lesssim 10\%$. Strongly enhanced damping, $\nu_{eff} \simeq 30\ \nu_{classical}$, of magnetoacoustic waves has, for example, been attributed to drift wave turbulence in a similar magnetized plasma column (Ritz et al., 1982). An enhancement factor of $\simeq$ 25 is required to explain the present experimental results by collisional damping. An enhanced damping can not, however, explain the observed shift of the resonance peak to a higher frequency.

(v) The theory of Sawley and Tran (1982) uses a fluid model for the plasma, and therefore neglects resonant wave-particle interactions. As discussed by Tran et al. (1982), the effect of ion cyclotron damping is expected, for the parameters considered, to be significant for only a very small range of frequencies in the vicinity of the cyclotron frequencies of the two ion species. However, since $\omega \simeq k_\parallel v_{th,e}$, electron

Landau damping may not only cause an increase in the power input to the plasma, but influence significantly the properties of the ion cyclotron wave. It is relatively straightforward to incorporate these kinetic effects into the theory of bounded ion cyclotron waves. The effect of electron Landau damping is illustrated by the example shown in Fig. 12. From this figure it can be seen that finite electron temperature effects modify significantly the frequency response of the plasma to the wave excitation considered. These effects broaden the resonance curves, as expected, and shift the resonance peak to a higher frequency. It appears possible to obtain quantitative agreement between theoretical predictions and experimental observations if electron Landau damping, and perhaps also enhanced collisional damping, are considered. A more detailed discussion of this subject will be presented in a future report.

V. CONCLUSIONS

The results presented in this report indicate that an eigenmode with $\omega \simeq \omega_{ci}$ has been excited in the plasma column of the LMP device. The magnetic component of the wavefields has been measured, indicating the electromagnetic nature of the excited mode. These fields have been excited via electromagnetic coupling from an external antenna. It appears that a favourable comparison of the observed wavefields with the predictions of theory can be made if electron Landau damping and enhanced collisional damping are considered.

The experimental results indicate that it is not possible to excite an ion cyclotron eigenmode, with the characteristics described by the theory of Sawley and Tran (1982), in the neon plasma created in the LMP device. This should be possible, however, if the electron temperature is lower (reducing the effect of electron Landau damping), and the density is more uniform (reducing the level of drift wave turbulence). A different choice of plasma source, e.g. a Q-device (necessitating a change in ion species), may provide a more suitable plasma for the investigation of a lightly-damped ion cyclotron eigenmode.

The fact that the measured magnetic field amplitudes are lower, and the resonance curves broader, than predicted by the theory of Sawley and Tran (1982) strongly suggests that the mode excited in the LMP device is not suitable for a study of the effect of the ponderomotive force. Since the experimental width of the resonance curves is about the same as the separation of the cyclotron frequencies of the two ion species, it appears unlikely that such a mode could efficiently differentiate between ions of different type. In addition, the total wavefield in the plasma has a sizeable, if not dominant, component due to the vacuum field of the antenna. This vacuum field has an unsuitable axial dependence for the proposed ponderomotive force experiment, due to the presence of only short regions of strong axial gradients. These considerations indicate that any modification of the ion concentration due to the excited wavefields would be extremely small. Since the measurement of the ion concentration using Doppler-free laser spectroscopy (Kohler, 1986) is extremely delicate with very limited resolution, detection of such small changes in the ion concentration would not be experimentally possible. It therefore appears that a much more feasible approach to investigate this effect of the ponderomotive force is that mentioned earlier in this report : utilizing the vacuum field of a suitably designed antenna. A preliminary experimental investigation of this alternative approach (Muggli, 1984) has shown considerably more promise.

ACKNOWLEDGEMENTS

The authors wish to thank the other members of the LMP group for the support they provided in the present work. This work was partially supported by the Fonds National Suisse de la Recherche Scientifique.

REFERENCES

Dodge, N.B., Kristiansen, M. and Dougal, A.A. (1966) Rev. Sci. Instrum. 37, 1455.

Festeau-Barrioz, M.-C. and Sawley M.L. (1985) Plasma Phys. and Contr. Fusion, 27, 641.

Kohler, P. (1986) "Doppler-free laser spectroscopy of a noble gas plasma" PhD Thesis No. 626, EPF-Lausanne.

Motz, H. and Watson, C.J.H. (1967) Adv. Electron. Electron Phys. 23, 153.

Muggli, P. (1984) "Effet non-linéaire dû à une onde électromagnétique dans un plasma magnétisé de basse densité" Diplôme Thesis, CRPP - Lausanne.

Ritz, Ch.P., Hoegger, B.A., Sayasov, Y.S., Schneider, H. and Vaucher, B.G. (1982) Helv. Phys. Acta, 55, 354.

Sawley, M.L. and Tran, M.Q. (1982) Lausanne Report LRP 206/82.

Sawley, M.L. (1985) Plasma Phys. and Contr. Fusion, 27, 957.

Tran, M.Q., Kohler, P., Paris, P.J. and Sawley, M.L (1982) Lausanne Report LRP 205/82.

Weibel, E.S. (1980) Phys. Rev. Lett. 44, 377.

FIGURE CAPTIONS

Fig. 1. Schematic diagram of the LMP device.

Fig. 2. Radial profiles of the electron density and temperature measured by Langmuir probes ($p_0=2.5\times10^{-4}$torr, $I_{cathode}$=1A). The density is calibrated using a 33 GHz microwave interferometer.

Fig. 3. (a) : Schematic diagram of the antenna and matching circuit; (b) : Detail of a coil module.

Fig. 4. Schematic diagram of the magnetic probe detection system.

Fig. 5. Frequency dependence of (a) the in-phase component, and (b) the out-of-phase component, of b_θ(r=1.25cm) measured midway between coil modules. ($p_0=2\times10^{-4}$ torr, I_{rf}=50A).

Fig. 6. Frequency dependence of the in-phase and out-of-phase components of b_θ(r=1.25cm) for a slightly lower value of B_0=2.85 kG. ($p_0=2\times10^{-4}$torr, $I_{cathode}$=2 A, I_{rf}=50A).

Fig. 7. Density dependence of the in-phase and out-of-phase components of b_θ(r=1.25cm). ($p_0=2\times10^{-4}$torr, I_{rf}=50A, f=220kHz)

Fig. 8. Neutral pressure dependence of the in-phase and out-of-phase components of b_θ(r=1.25cm). ($I_{cathode}$=1A, I_{rf}=50A, f=220 kHz)

Fig. 9. Radial profiles of (a) the in-phase component, and (b) the out-of-phase component of b_θ. ($p_0=2\times10^{-4}$torr, I_{rf}=50A, f=220kHz)

Fig. 10. Radial profiles of (a) the in-phase component, and (b) the out-of-phase component of b_θ. ($p_0=2\times10^{-4}$torr, $I_{cathode}=1A$, $I_{rf}=50A$)

Fig. 11. Frequency dependence of, top, power input to the plasma for the n = 4 axial mode, and bottom, corresponding $b_\theta(r=1.25cm)$ at an axial antinode of the wavefield. At the right is shown the real part (in-phase component) and at the left is shown the imaginary part (out-of-phase component). These curves were calculated from theory, including ion-neutral collisions as the sole damping mechanism. ($n_e=10^{11}$ cm^{-3}, $\nu_{in}=5kHz$ corresponding to $n_n\simeq6\times10^{12}cm^{-3}$, $I_{rf}=50A$)

Fig. 12. Same as Fig. 11, except that both ion-neutral collisions and electron Landau damping are included in the theory. ($n_e=10^{11}cm^{-3}$, $T_e=5eV$, $\nu_{in}=5kHz$, $I_{rf}=50A$)

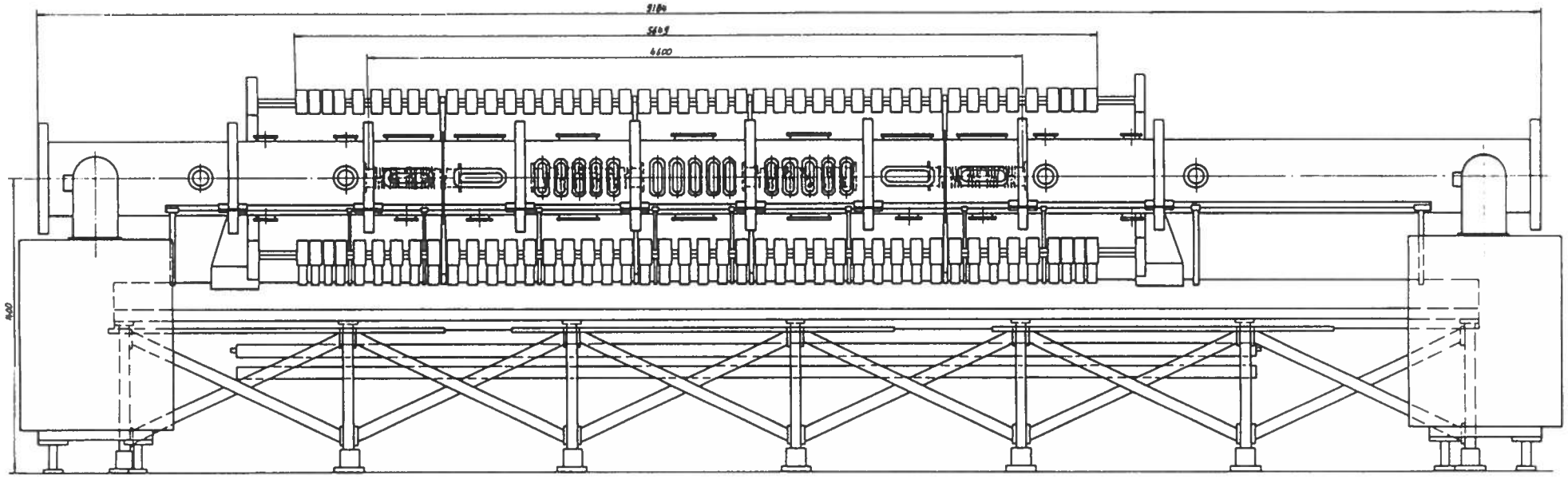

Figure 1

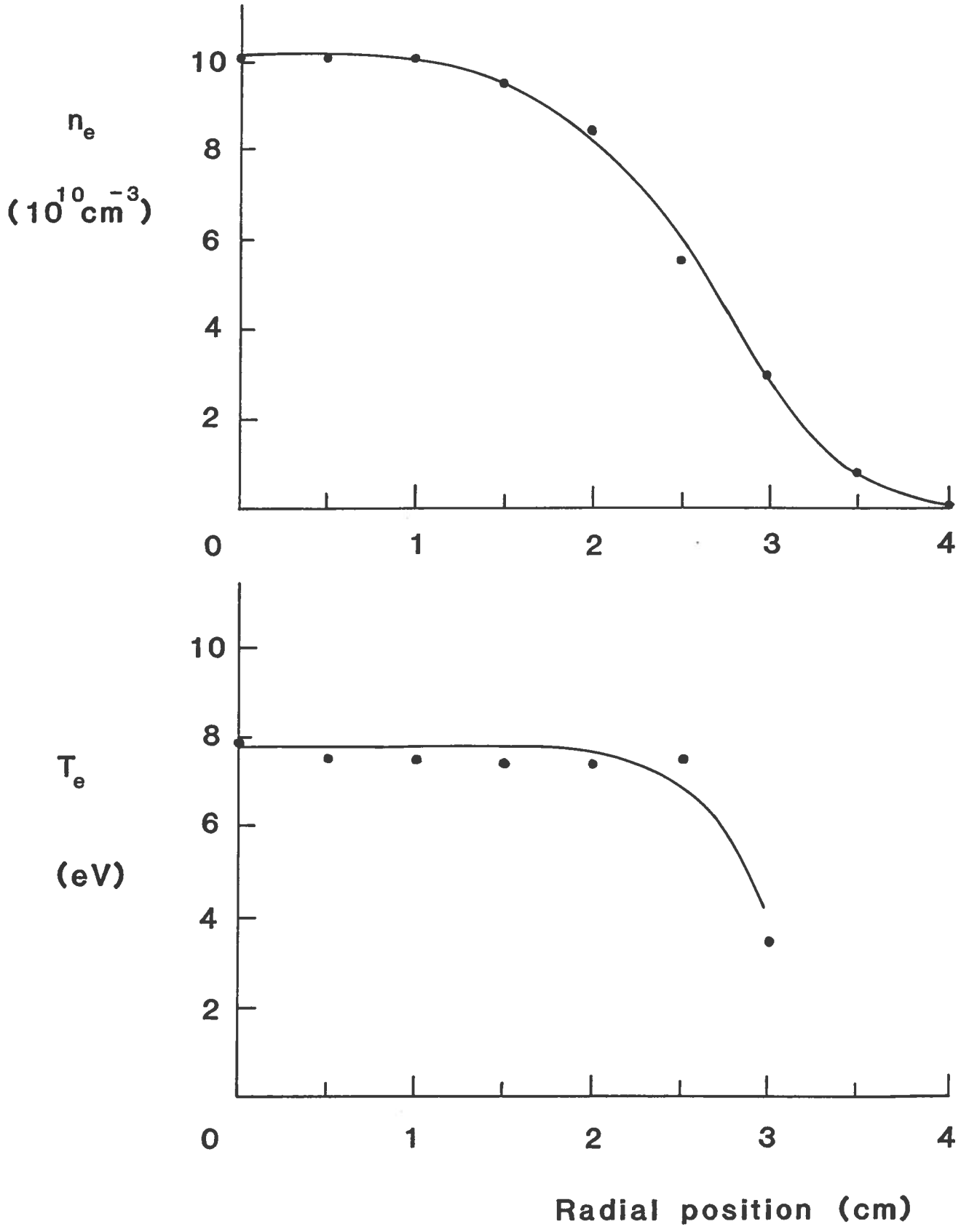
n_e
$(10^{10} cm^{-3})$
10
8
6
4
2
0
1
2
3
4
T_e
(eV)
10
8
6
4
2
0
1
2
3
4
Radial position (cm)

Figure 2

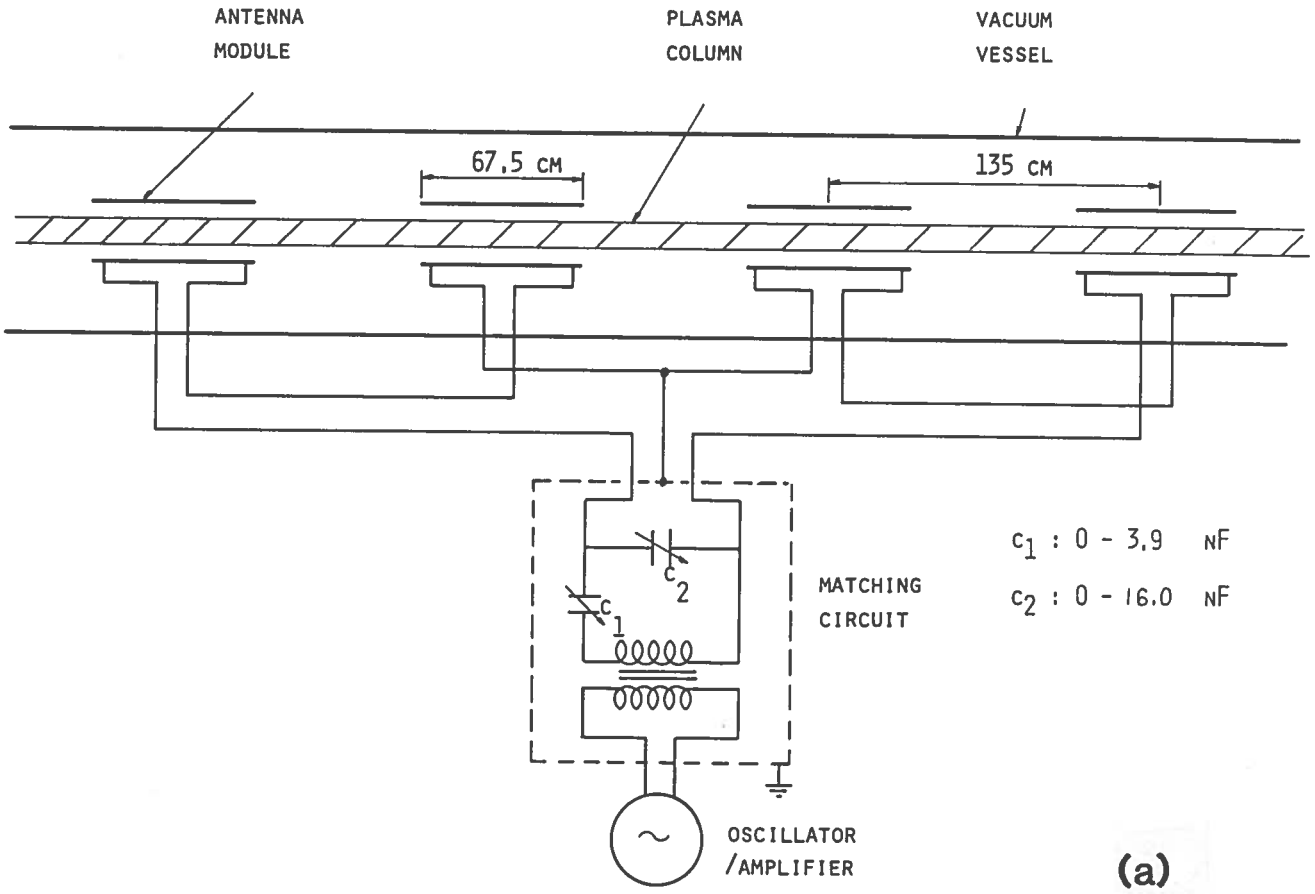
ANTENNA
MODULE
PLASMA
COLUMN
VACUUM
VESSEL
67.5 CM
135 CM
C2
C1
MATCHING
CIRCUIT
C1 : 0 - 3.9 NF
C2 : 0 - 16.0 NF
OSCILLATOR
/AMPLIFIER
(a)

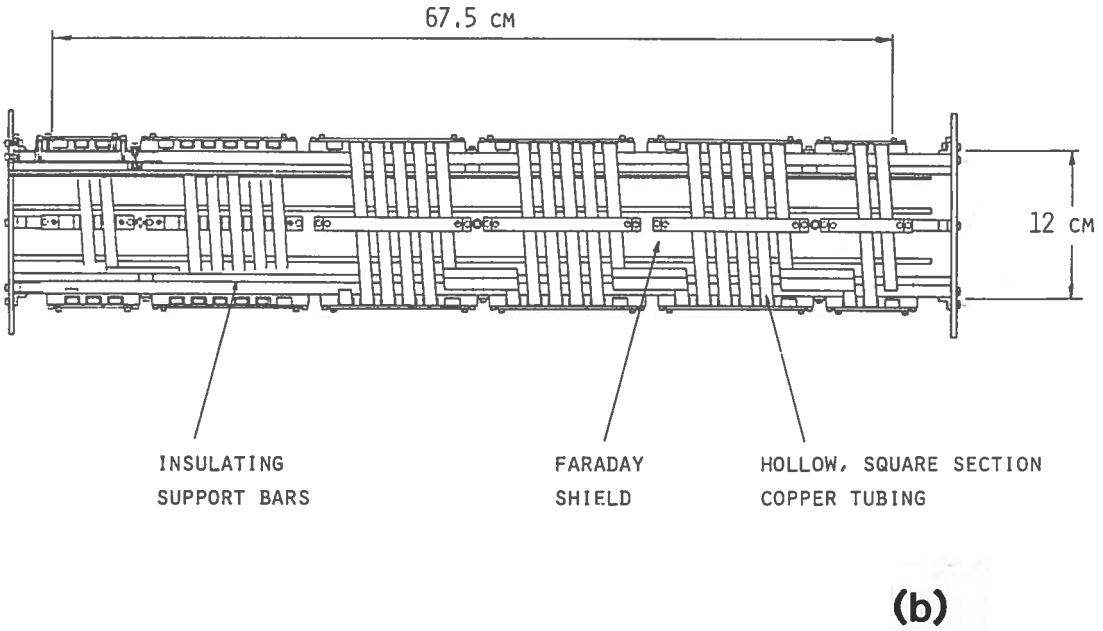
67.5 CM
12 CM
INSULATING
SUPPORT BARS
FARADAY
SHIELD
HOLLOW, SQUARE SECTION
COPPER TUBING
(b)

Figure 3

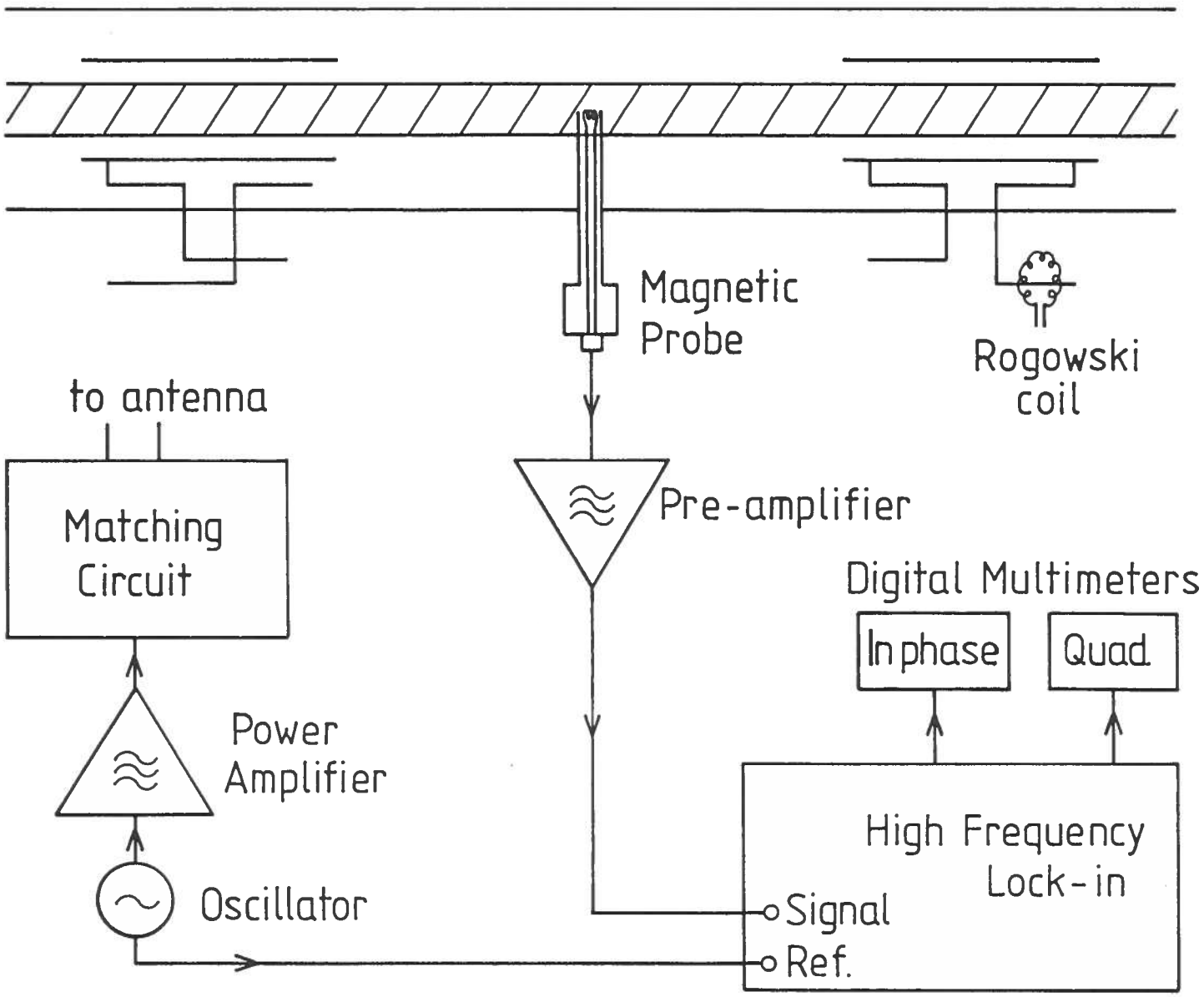
Magnetic
Probe
Rogowski
coil
to antenna
Matching
Circuit
Pre-amplifier
Digital Multimeters
In phase
Quad
Power
Amplifier
High Frequency
Lock-in
Oscillator
Signal
Ref.

Figure 4

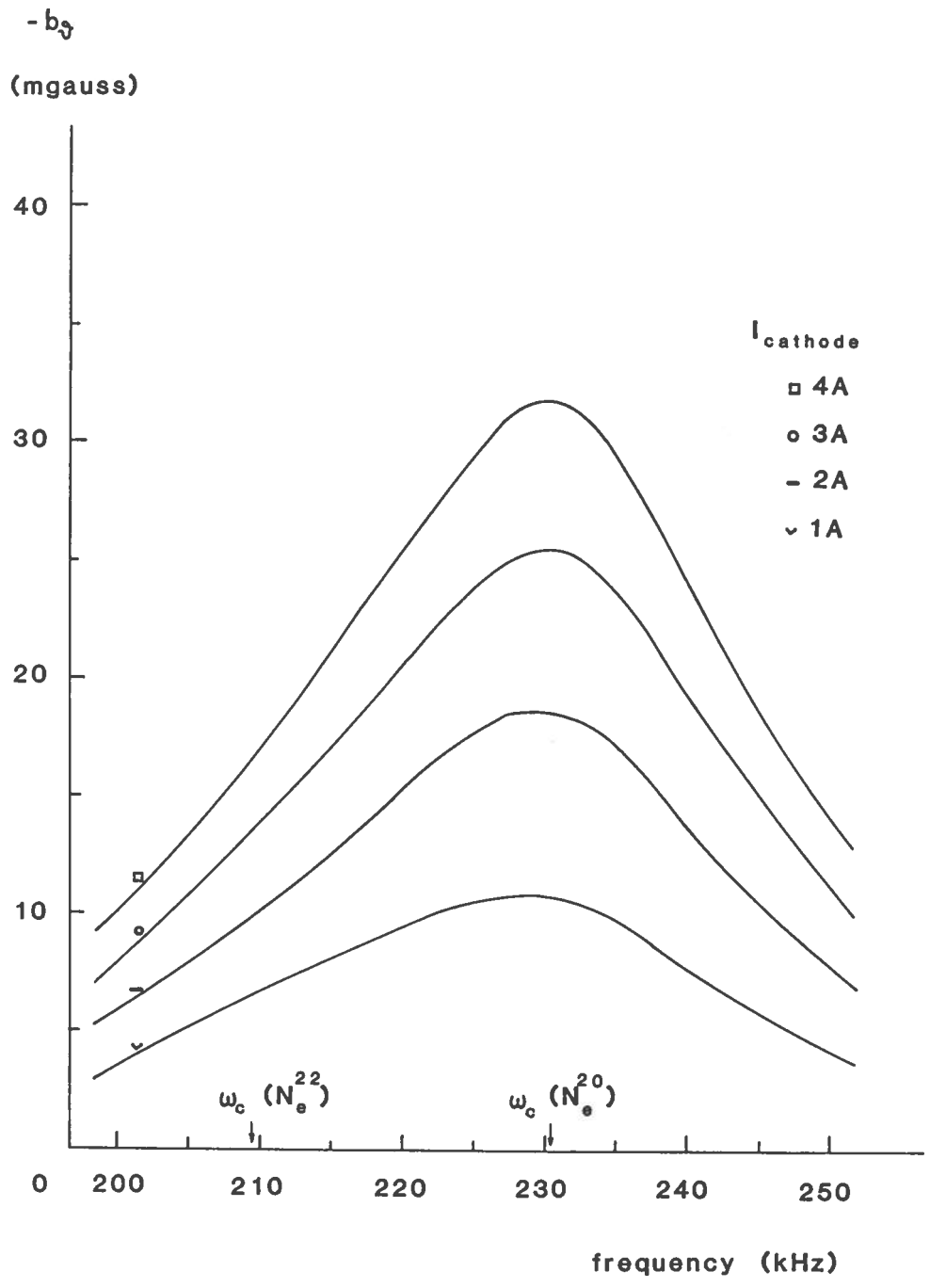
- b_ϑ
(mgauss)
40
30
20
10
0
200
210
220
230
240
250
frequency (kHz)
$I_{cathode}$
4A
3A
2A
1A
ω_c (N_e^{22})
ω_c (N_e^{20})

Figure 5(a)

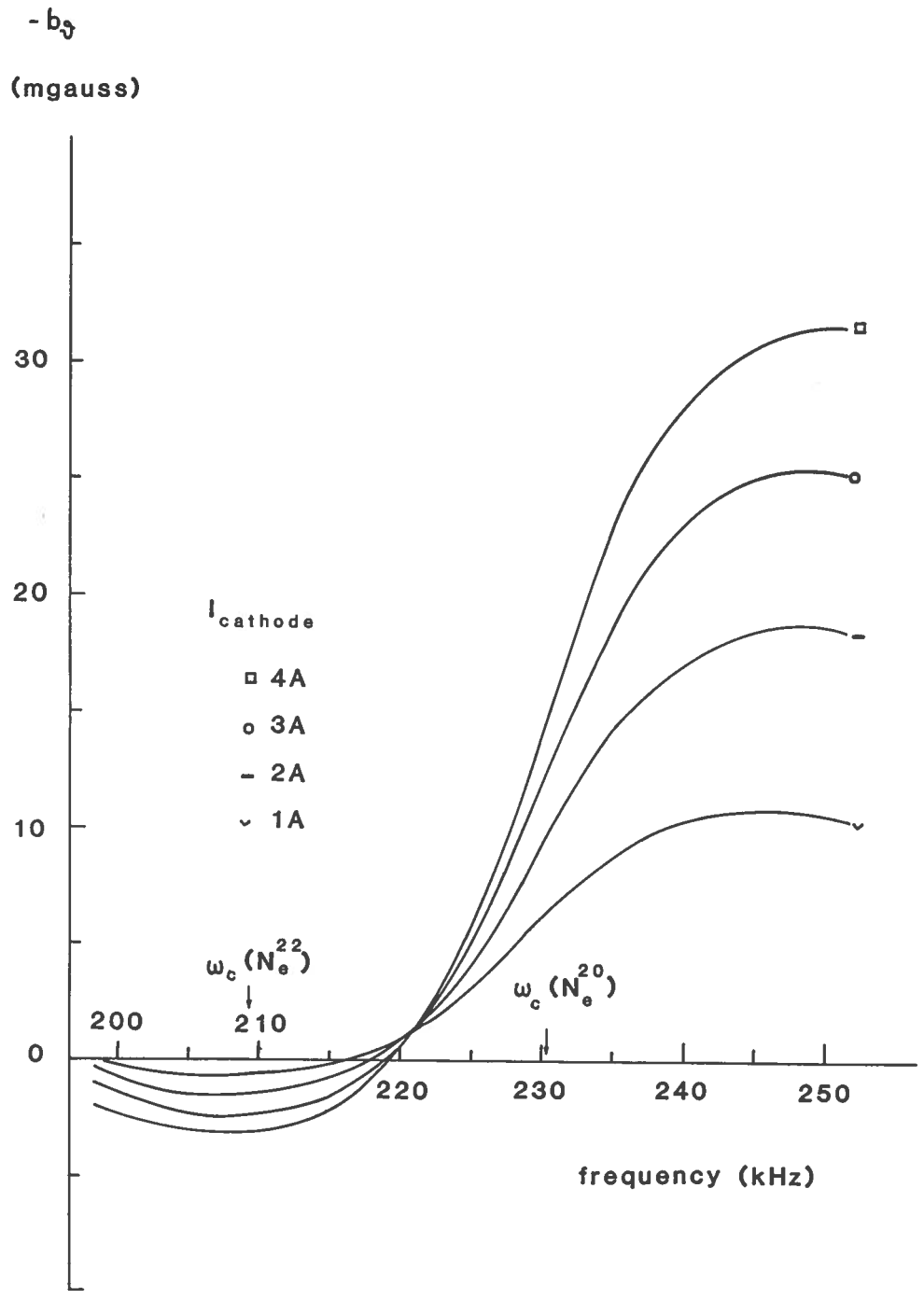
- b_ϑ
(mgauss)
30
20
10
0
$I_{cathode}$
4A
3A
2A
1A
$\omega_c (N_e^{22})$
$\omega_c (N_e^{20})$
200
210
220
230
240
250
frequency (kHz)

Figure 5(b)

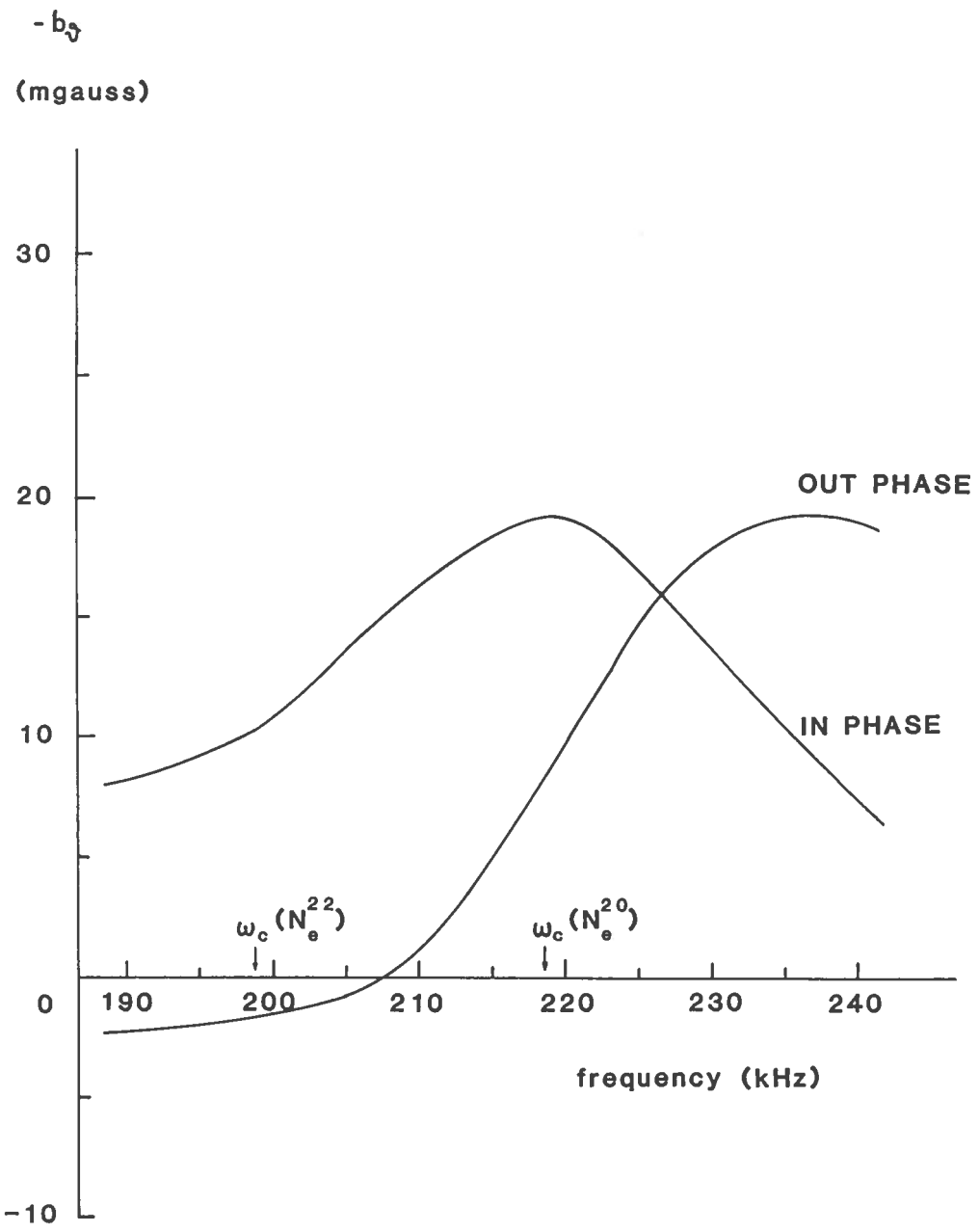
- b_ϑ
(mgauss)
30
20
10
0
-10
OUT PHASE
IN PHASE
$\omega_c(N_e^{22})$
$\omega_c(N_e^{20})$
190
200
210
220
230
240
frequency (kHz)

Figure 6

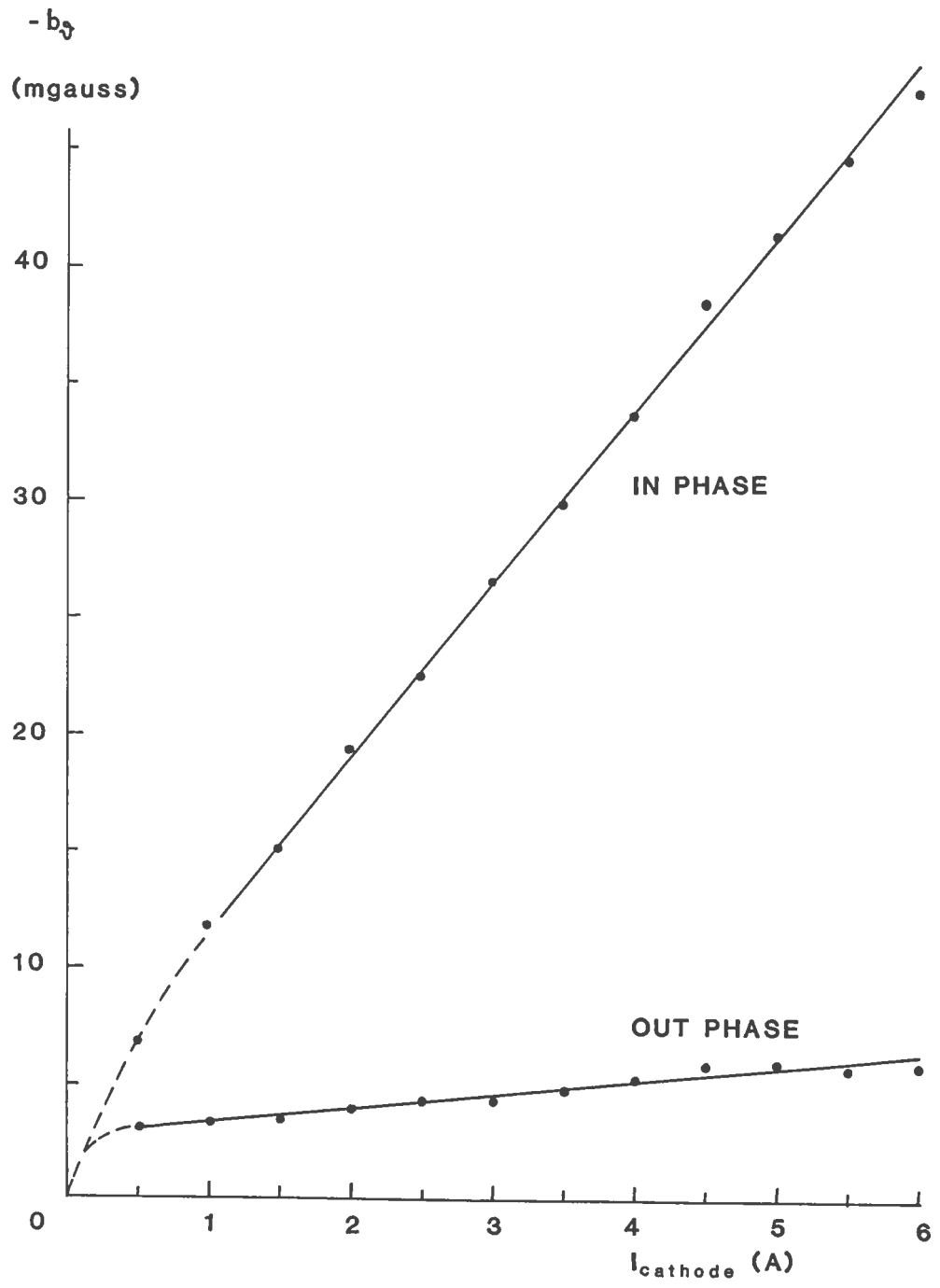

Figure 7

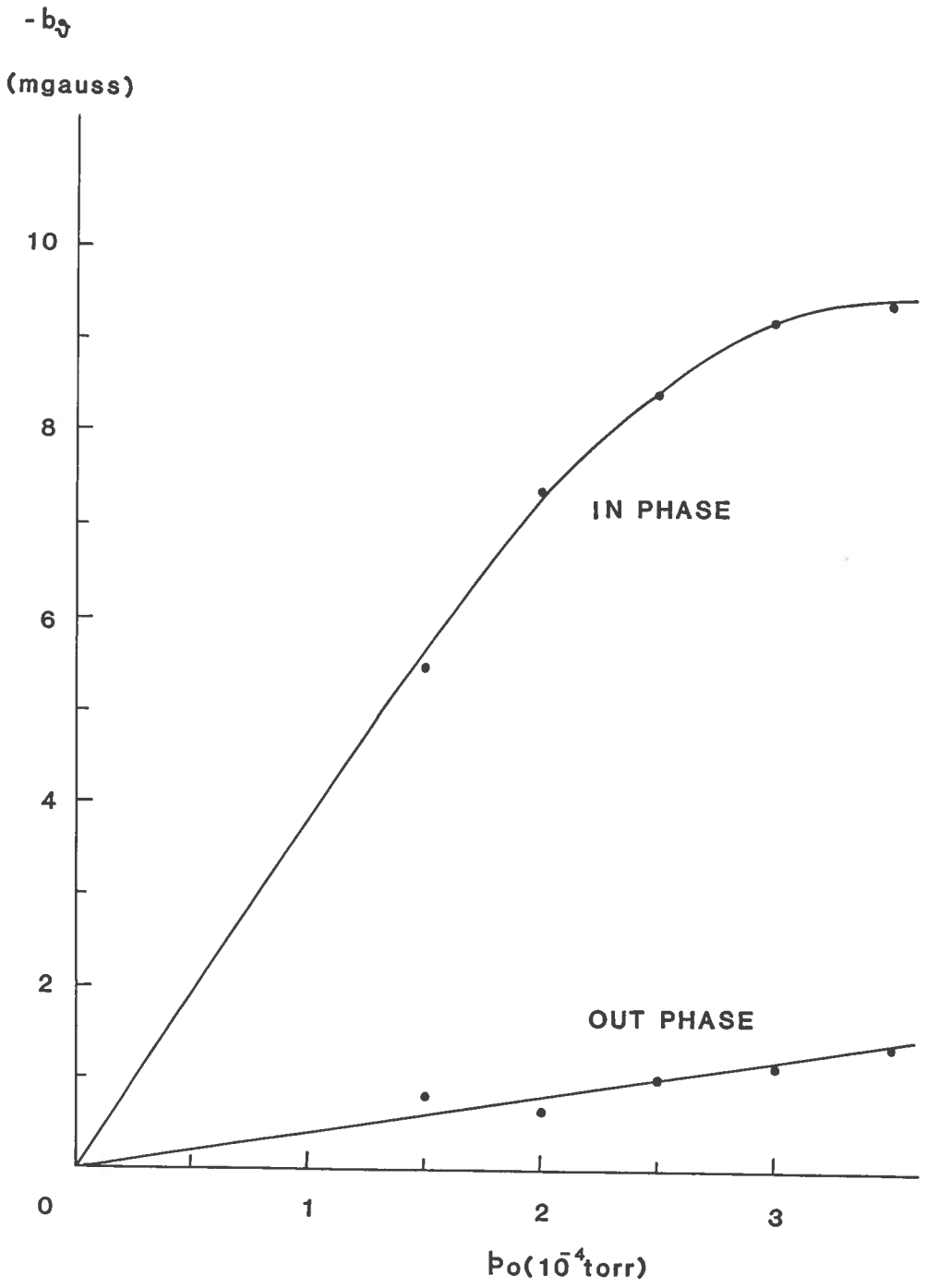

Figure 8

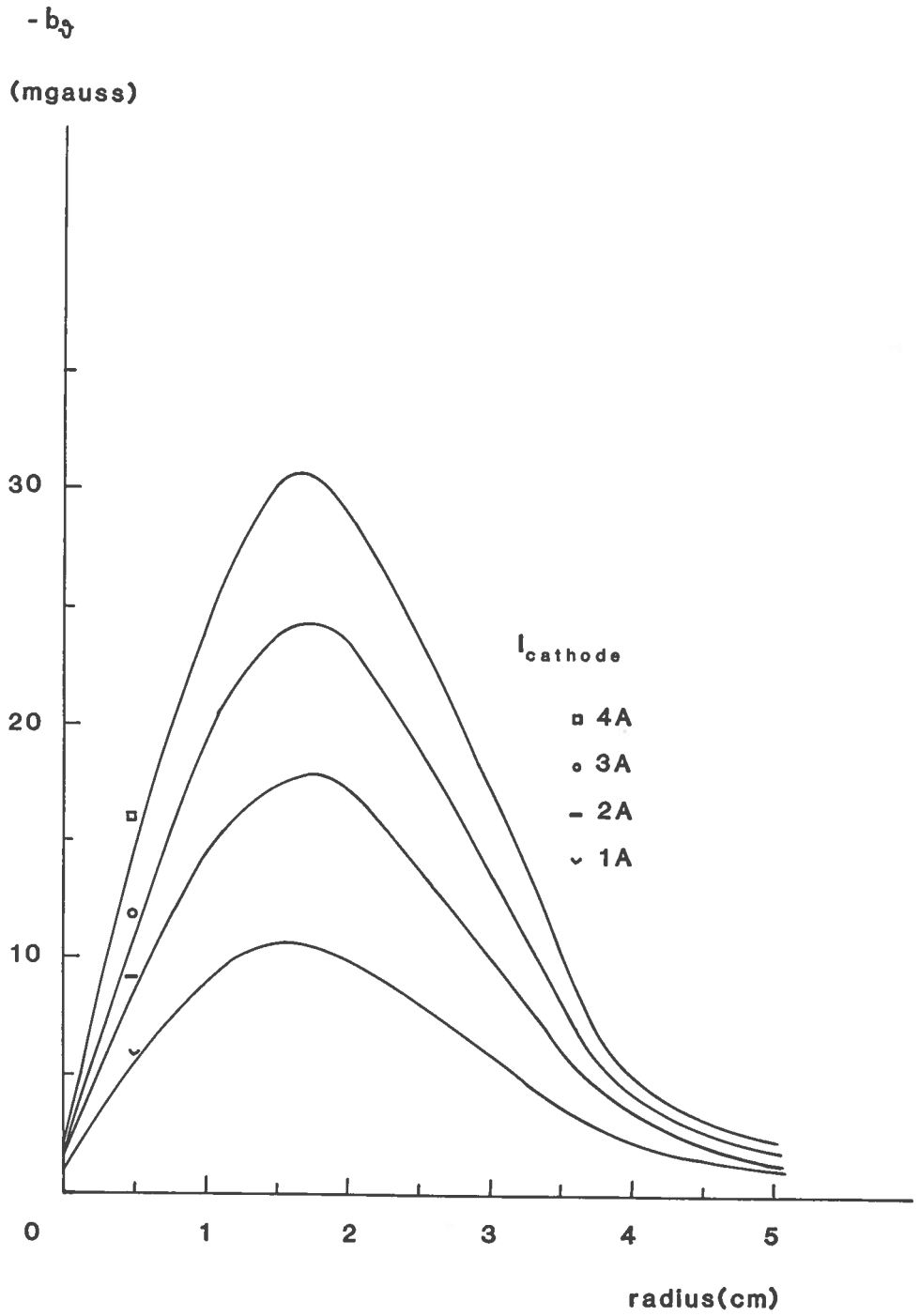
- b_ϑ
(mgauss)
30
20
10
0
1
2
3
4
5
radius(cm)
$I_{cathode}$
4A
3A
2A
1A

Figure 9(a)

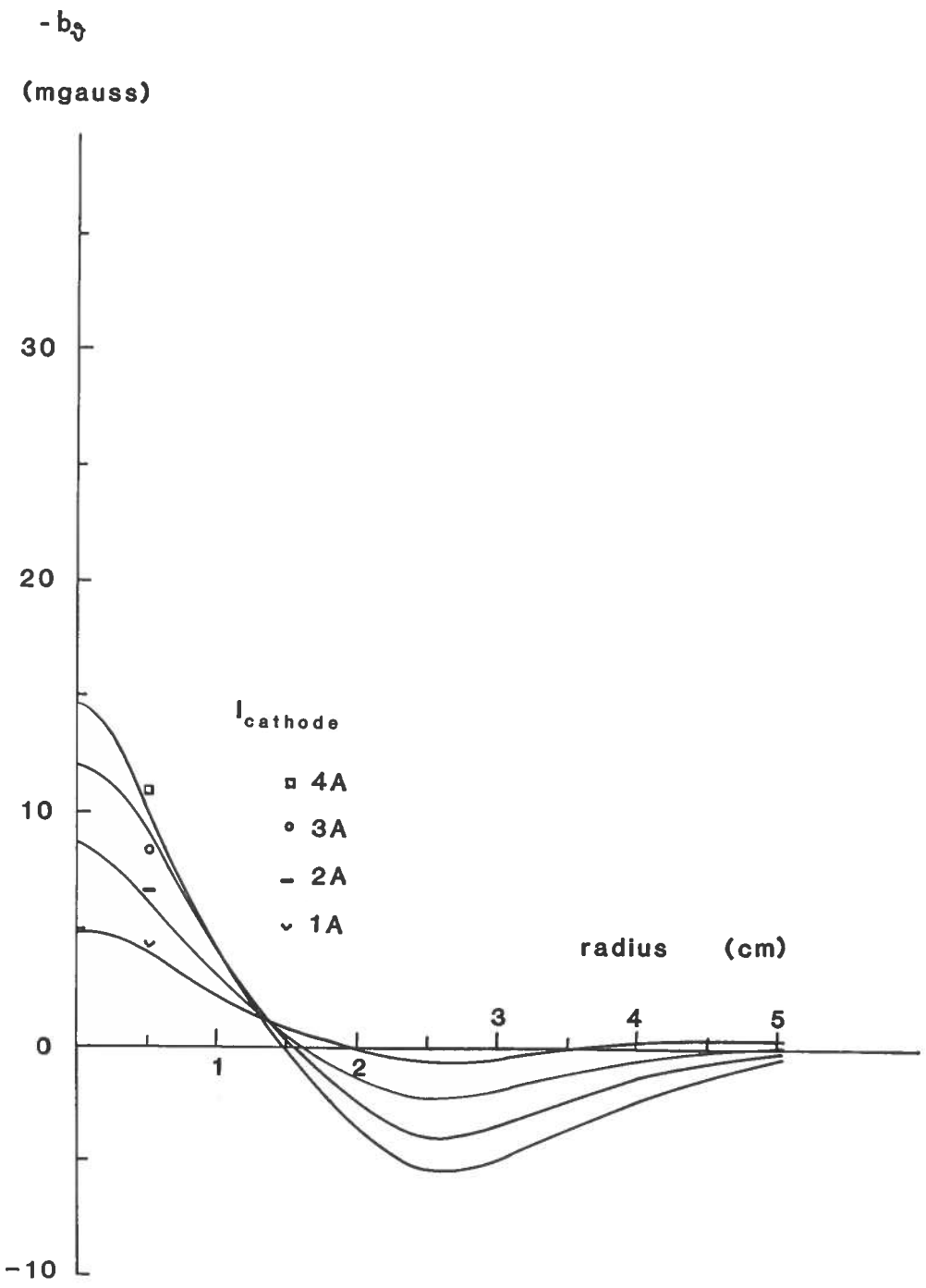
- b_ϑ
(mgauss)
30
20
10
0
−10
$I_{cathode}$
4A
3A
2A
1A
radius (cm)
1
2
3
4
5

Figure 9(b)

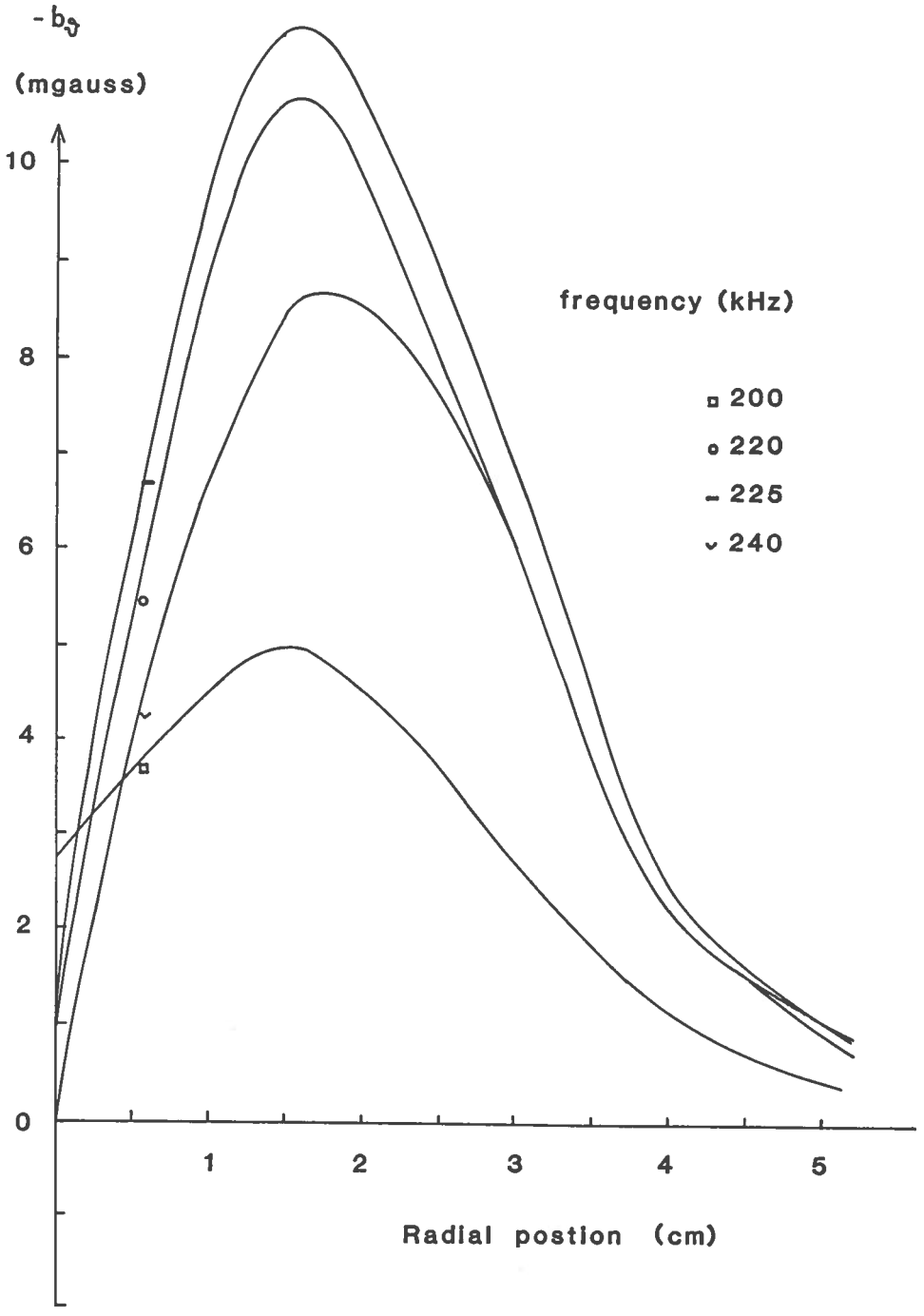
- b_ϑ
(mgauss)
10
8
6
4
2
0
1
2
3
4
5
Radial postion (cm)
frequency (kHz)
200
220
225
240

Figure 10(a)

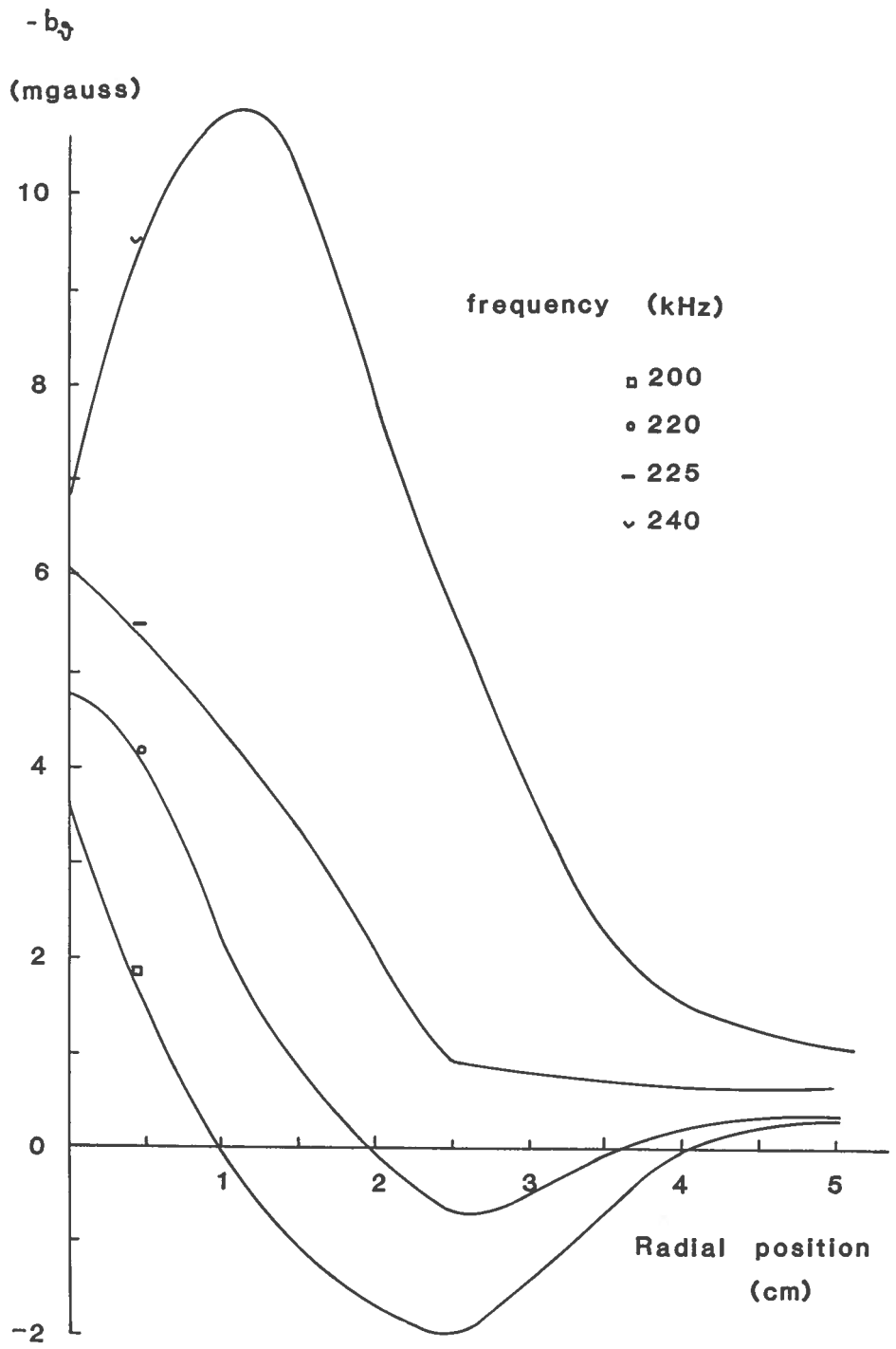
- b_ϑ
(mgauss)
10
8
6
4
2
0
-2
1
2
3
4
5
frequency (kHz)
200
220
225
240
Radial position
(cm)

Figure 10(b)

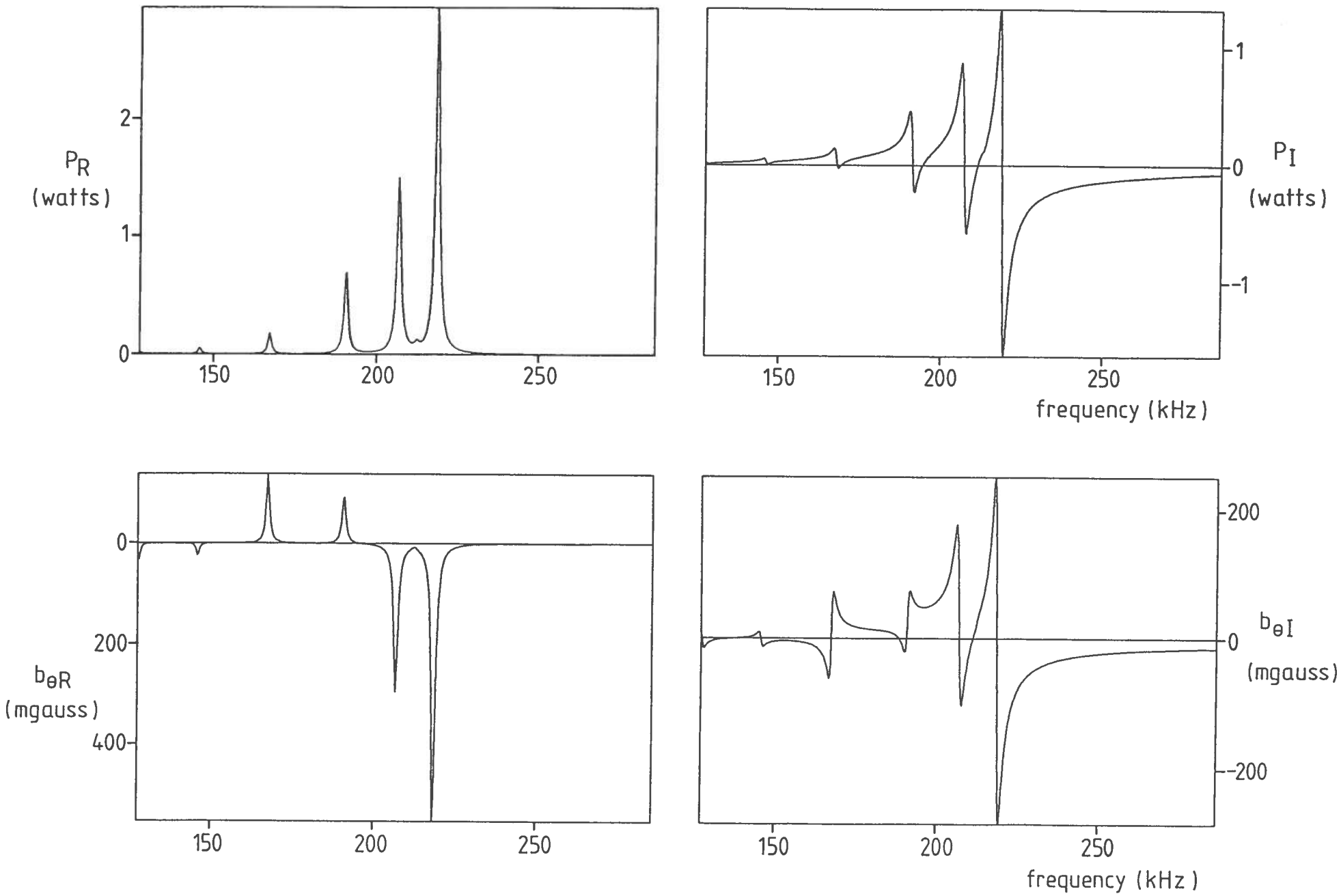
P_R
(watts)
2
1
0
150
200
250
1
0
−1
P_I
(watts)
frequency (kHz)
b_{eR}
(mgauss)
0
200
400
200
0
−200
b_{eI}
(mgauss)
frequency (kHz)

Figure 11

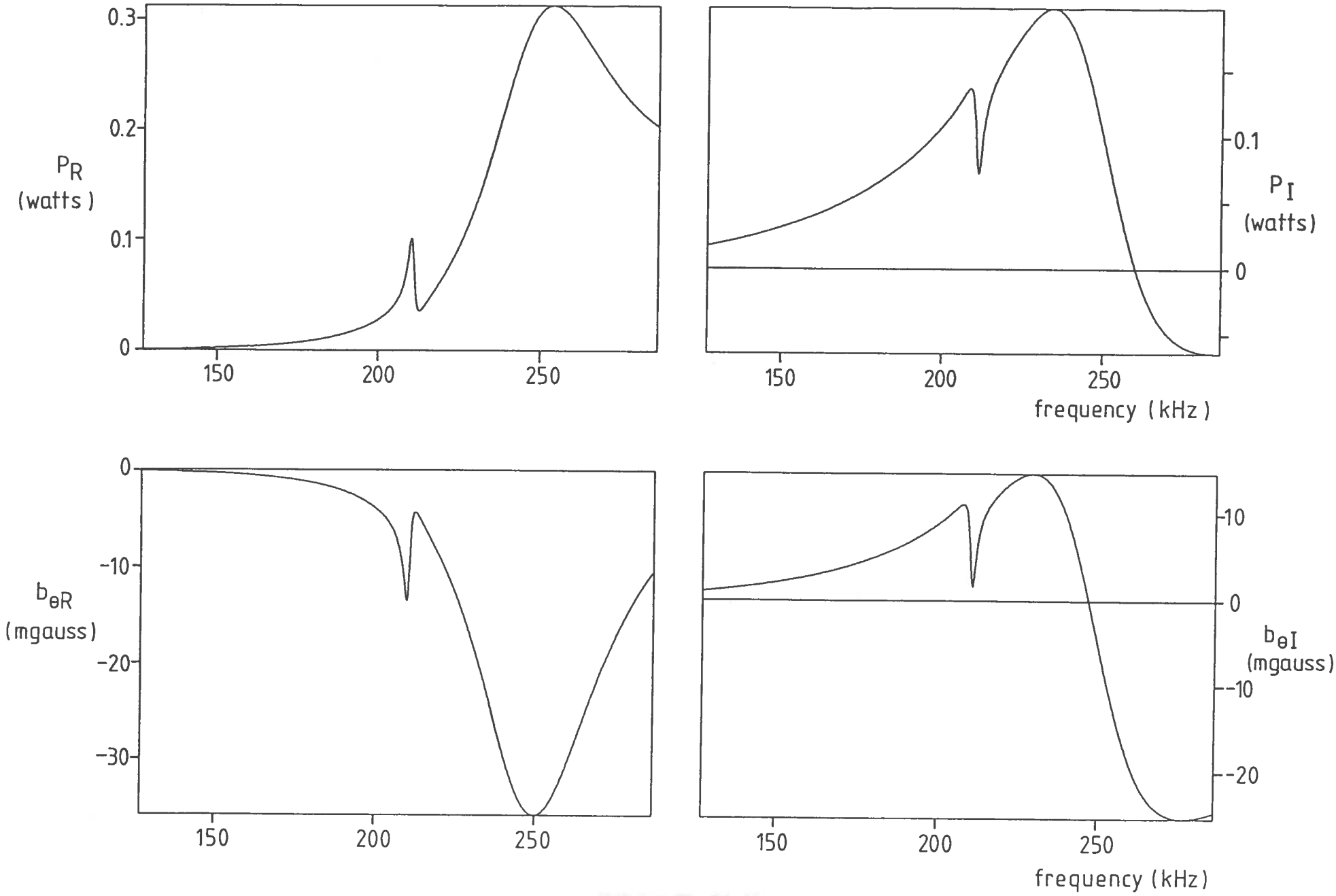
0.3
0.2
0.1
0
P_R
(watts)
150
200
250
0.1
0
P_I
(watts)
frequency (kHz)
0
-10
-20
-30
$b_{\theta R}$
(mgauss)
10
0
-10
-20
$b_{\theta I}$
(mgauss)
frequency (kHz)

Figure 12